

ARTICLE

Received 14 May 2014 | Accepted 23 Jun 2014 | Published 28 Jul 2014

DOI: 10.1038/ncomms5484

Interlocked loops trigger lineage specification and stable fates in the *Drosophila* nervous system

Hakima Flici^{1,2,3,4,*†}, Pierre B. Cattenoz^{1,2,3,4,*}, Orban Komonyi^{1,2,3,4}, Pietro Laneve^{1,2,3,4,†}, Berra Erkosar^{1,2,3,4,†}, Omer F. Karatas^{1,2,3,4,†}, Heinrich Reichert⁵, Sara Berzsenyi^{1,2,3,4,†} & Angela Giangrande^{1,2,3,4}

Multipotent precursors are plastic cells that generate different, stable fates at the correct number, place and time, to allow tissue and organ formation. While fate determinants are known to trigger specific transcriptional programs, the molecular pathway driving the progression from multipotent precursors towards stable and specific identities remains poorly understood. Here we demonstrate that, in *Drosophila* neural precursors, the glial determinant glial cell missing (*Gcm*) acts as a 'time bomb' and triggers its own degradation once the glial programme is stably activated. This requires a sequence of transcriptional and post-transcriptional loops, whereby a *Gcm* target first affects the expression and then acetylation of the fate determinant, thus controlling *Gcm* levels and stability over time. Defective homeostasis between the loops alters the neuron:glia ratio and freezes cells in an intermediate glial/neuronal phenotype. In sum, we identify an efficient strategy triggering cell identity, a process altered in pathological conditions such as cancer.

¹Institut de Génétique et de Biologie Moléculaire et Cellulaire, 67404 Illkirch, France. ²Centre National de la Recherche Scientifique, UMR7104, 67404 Illkirch, France. ³Institut National de la Santé et de la Recherche Médicale, U964, 67404 Illkirch, France. ⁴Université de Strasbourg, 67404 Illkirch, France. ⁵Biozentrum University of Basel, Klingelbergstrasse 50/70CH, 4056 Basel, Switzerland. * These authors contributed equally to this work. † Present addresses: School of Natural Sciences & Regenerative Medicine Institute (REMEDI), National University of Ireland, Galway, Ireland (H.F.); Center for Life Nano Science@Sapienza, Istituto Italiano di Tecnologia 00161 Rome, Italy (P.L.); Department of Medical Genetics, Cerrahpasa Medical School, Istanbul University, Istanbul, Turkey (O.F.K.); Functional Genomics, Institute of Lyon (IGFL), UMR5242 CNRS/ENS Lyon, 32 Avenue Tony Garnier, F-69364 Lyon Cedex 07, France (B.E.); BioTalentum Ltd, Gödöllő 2100, Hungary (S.B.). Correspondence and requests for materials should be addressed to A.G. (email: angela@igbmc.fr).

Lineage specification, the process that restricts the potential of multipotent precursors, involves the implementation of a novel transcriptional programme, however, many determinants are only expressed transiently, begging questions as to the molecular pathway ensuring stable identity and terminal differentiation. To understand how this is achieved *in vivo*, we used a simple model. The *Drosophila* central nervous system develops from stem cell-like precursors called neuroblasts (NBs) that produce neurons and glia¹. The *glide/gcm* gene (glial cell deficient/glial cell missing, referred to as *gcm*) codes for a transiently expressed transcription factor that is necessary and sufficient for the differentiation of all lateral embryonic glia. Lack of Gcm transforms most lateral glia into neurons, whereas its forced expression converts neural precursors into glia^{2–5}. Thus, Gcm provides an ideal tool to analyse the pathway underlying lineage specification.

gcm activates several targets that implement the glial fate^{6–8} including Repo (reversed polarity), a homeodomain transcription factor permanently expressed in all lateral glia^{9–11}. Interestingly, Gcm and Repo boost their own expression on autoregulation^{4,12} and transiently coexist^{2,3,9,10,13,14}. Thus, we hypothesized that Repo acts as a molecular relay, regulating the threshold and dynamic accumulation of Gcm that is necessary for gliogenesis.

We show that *Drosophila* Creb binding protein (dCBP), a histone acetyltransferase (HAT)¹⁵ regulates Gcm stability. dCBP interacts with and triggers the acetylation of Repo and Gcm, which also interact with each other and the three factors are shared components of two interlocked loops. On the one hand, Repo positively regulates *gcm* gene expression and dCBP induces Gcm stability, on lysine acetylation. On the other hand, Repo induces Gcm degradation in a dosage-dependent manner and dCBP enhances Repo-mediated Gcm degradation. Thus, dCBP and Repo positively regulate Gcm transcriptionally at the beginning of the gliogenic pathway, when Repo starts being expressed, and negatively regulate it posttranscriptionally at a later stage, when Repo accumulates at high levels. The intimate link between the trigger and the consolidator of the glial fate ensures the proper neuron:glia ratio and a stable glial identity. Breaking the homeostasis alters the ratio and freezes cells in a neuronal–glial intermediate state.

In sum, this work identifies the molecular network controlling glial specification and the mode of action of the fate determinant.

Results

Gcm and Repo positively control *gcm* expression. Cell specification is a binary decision, a type of process that often relies on threshold levels of signalling molecules. We thus dissected the quantitative control of the glial determinant and its impact on the process. Gcm has a dosage-dependent gliogenic effect¹⁶ (Fig. 1a,b top panels) and positively autoregulates^{4,12} (see the induction of endogenous transcripts on Gcm ectopic expression in the neurogenic region, *scabrous-gal4* (*sca*) driver; Fig. 1c). Moreover, autoregulation depends on Gcm levels (Fig. 1a,b), as seen by following β -galactosidase (β gal) labelling in embryos expressing increasing *gcm* doses in a *gcm*^{rA87} line, which expresses the *lacZ* gene under the control of the *gcm* promoter^{4,12} (Supplementary Fig. 1a). Finally, using a strong *gcm* transgene leads to an even further increase in the number of ectopic glia and in the proportion of glial cells that show Gcm autoregulation (the large majority if not all Repo(+) cells are β gal(+) as well: Fig. 1a,b,d). Thus, *gcm* autoregulation is dosage dependent as is the potential to convert neurons in glia (see the number of neurons, Supplementary Fig. 1b–d).

We next asked whether the Gcm target Repo feeds back and controls *gcm* autoregulation, as suggested by the finding that

ectopic β gal appears later than ectopic Repo (Fig. 1e,f). The levels of *gcm* RNA are indeed reduced in *repo* compared to wild-type (WT) embryos (Fig. 2a), as are the levels of β gal in a *gcm*^{rA87} *repo* background (Supplementary Fig. 1e). Similarly, *gcm* autoregulation is also reduced in *gcm*^{rA87} *repo* embryos ectopically expressing Gcm (Fig. 2c) compared with control embryos (Fig. 2b).

The positive effects of Repo may have at least three explanations: (1) Gcm needs Repo as a cofactor to act on its own promoter, (2) Repo directly binds the *gcm* promoter to activate it or (3) both processes contribute to induction. On transfecting *Drosophila* S2 cells, which express no endogenous *gcm* or *repo*, we found that Repo induces the expression of a reporter gene driven by the *gcm* promoter (Fig. 2f columns 1,3), which contains nine Repo binding sites (RBS)^{9,11} that are conserved in the *Drosophila* species (UCSC browser, <http://genome.ucsc.edu/>) (Fig. 2d,e). Each RBS was cloned in a luciferase reporter vector and co-transfected in S2 cells in the presence or absence of Repo (Sites 8–9 were cloned in the same vector, due to their close proximity). Repo induces significant expression of the luciferase reporters carrying RBS 1, 4, 7, 8, 9 in their promoters (Fig. 2g). RBS 1 presents the strongest induction, with a 3.2 fold increase of the luciferase activity, comparable to previous results obtained with a luciferase reporter containing two RBS¹¹. To assess *in vivo* the binding of Repo to the promoter of *gcm*, a ChIP targeting Repo was carried out in stage 11 WT embryos. RBS 1 and RBS 4 are significantly enriched, 3 and 4.2 folds respectively (Fig. 2h), at levels comparable to those obtained using the same approach on other transcription factors^{17–19}. The other active sites seem moderately or not significantly enriched, which may be due to weak binding. Finally, none of the sites that are silent in S2 cells are enriched in our ChIP assay. *In vitro* experiments specifically performed on RBS 1 also confirm DNA binding (Supplementary Fig. 1f).

Thus, Repo can directly bind the *gcm* promoter and maintains *gcm* expression.

Repo promotes Gcm degradation via the proteasome. Gcm may use its direct target Repo to reach the threshold levels required for gliogenesis. If that were the case, ectopic Repo expression should reinforce the gliogenic effects of *gcm*. Surprisingly, however, the number of *gcm* autoregulating cells on Repo and Gcm ectopic coexpression drastically decreases compared with that found in control embryos (Fig. 3a,b bottom panels), as is the number of ectopic Repo(+) cells (Fig. 3a,b top panels). Similar phenotypes were also obtained with the tagged transgene (*gcmFlag*) (Supplementary Fig. 2a) that allows discriminating endogenous from exogenous *gcm* expression. These effects are not due to Gal4 titration induced by using two reporters (*gcm* + *repo*) rather than one (*gcm*), since coexpression of green fluorescent protein (GFP) and Repo using the same driver does not reduce GFP expression (Supplementary Fig. 2c–e). Thus, Repo exerts opposite effects on *gcm*, and we speculated that Repo negatively controls *gcm* at posttranscriptional level.

Repo does not seem to affect *gcm* messenger RNA steady-state stability, as assessed by quantitative PCR (qPCR) analysis in *sca* > GFP + *gcmFlag* and in *sca* > GFP + *gcmFlag* + *repo* embryos. The levels of ectopic *gcm* transcripts, which do not depend on autoregulation, are similar in the two genotypes (Supplementary Fig. 2g left columns). The levels of the endogenous transcripts are lower in *sca* > GFP + *gcmFlag* + *repo* than in *sca* > GFP + *gcmFlag* embryos (Supplementary Fig. 2g right columns), suggesting that Repo negatively affects the Gcm/GcmFlag proteins and thereby autoregulation.

To verify the role of Repo on the Gcm protein, we performed western blot (WB) analyses using embryos of the above genotypes

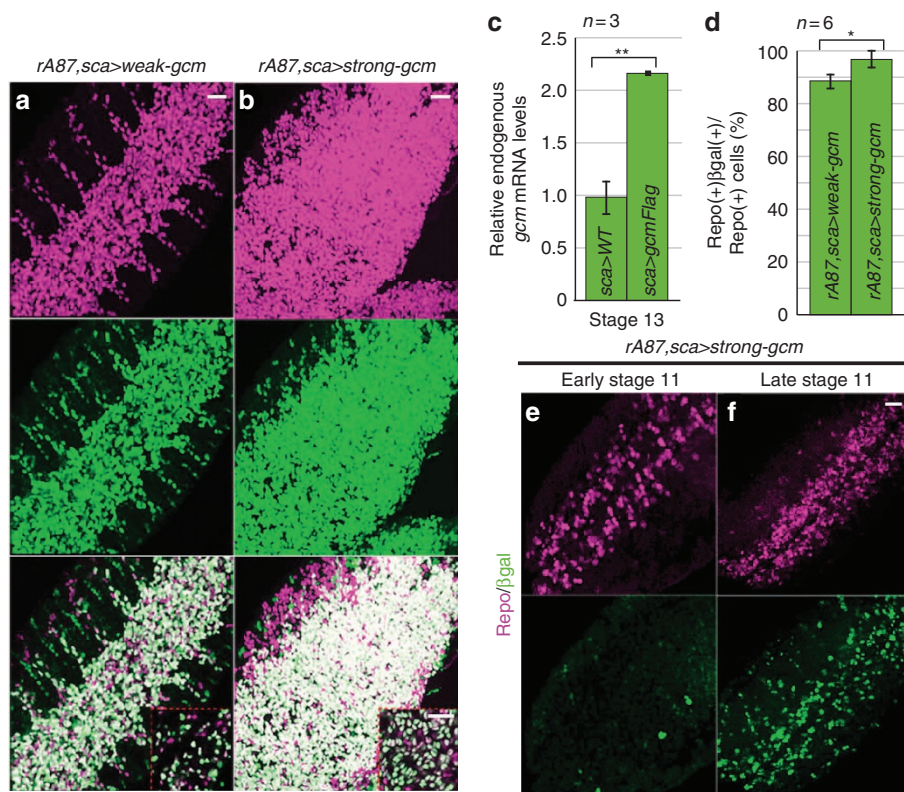


Figure 1 | *gcm*-positive autoregulation is Gcm dosage dependent. (a, b) Stage 16 embryos IHC for the nuclear glial marker Repo (magenta, unless specified) and *gcm* autoregulation marker (β gal, green, unless specified). All figures show confocal projections of ventral views, unless specified. Insets show magnifications of a region of interest, single sections. The *UAS-gcm* line shown in a was used throughout the work, unless specified. (c) Mean levels of the endogenous *gcm* transcripts in *sca>WT* and *sca>gcmFlag* embryos (three qPCR assays, primers in Supplementary Table 1). (d) Percentage of Repo(+), β gal(+) cells in three segments of the embryonic VNC. *n*, number of embryos. (e, f) Repo and β gal expression at mentioned embryonic stages. In all figures: st, embryonic stages; error bars indicate \pm s.e.m.; *P*-value are estimated using student test and **P*-value (0.05–0.01); ***P*-value (0.01–0.001); ****P*-value < 0.001; NS, nonsignificant *P*-value (> 0.05); exact values for all *P*-values are detailed in Supplementary Note 1, scale bars, 20 μ m.

at stage 11 (Supplementary Fig. 2f, mid and left lanes), when Repo is already detected (Supplementary Fig. S2d). Gcm accumulates at lower levels in embryos ectopically coexpressing Gcm and Repo than in embryos that ectopically express only Gcm (histogram in Fig. 3c), also confirmed by measuring total signal intensity on Flag immunohistochemistry (IHC) assays (Fig. 3d)²⁰. No stable antibody against Gcm is currently available to monitor endogenous Gcm but the fact that the tag does not affect Gcm behaviour (Supplementary Fig. 2a) strongly suggests that the endogenous Gcm as well is destabilized and rapidly eliminated on Repo forced expression.

Since the ubiquitin proteasome is involved in degrading many proteins including Gcm^{21,22}, we asked whether Repo acts at least in part via this pathway. Gcm and Repo regulate their own expression and cross regulate, which makes it difficult to disentangle transcriptional from posttranscriptional regulation in embryos. We therefore transfected S2 cells with *pAct-gcmFlag* and *pAct-repo* expression constructs and found that Repo reduces Gcm levels in a dosage-dependent manner (Fig. 3e, f). We can exclude translation competition because Gcm and GFP cotransfection does not trigger the same effect. The above data also explain why the expression of the *gcm* reporter does not significantly increase in S2 cells coexpressing Repo and Gcm compared with those induced by the expression of Repo or Gcm alone (Fig. 2f column 4 versus 2, 3).

Finally, treatment with the MG132 proteasome inhibitor alleviates the Repo-dependent decrease of Gcm levels (Fig. 3e, f). The partial rescue could be due to the fact that Repo-dependent

but proteasome-independent pathways are also involved or that the levels of the inhibitor are not sufficient. Nevertheless, these results confirm that Repo affects Gcm levels via the proteasome.

dCBP stabilizes Gcm. The above data strongly suggest that Repo controls the timely decay of Gcm prompting us to ask what controls Gcm stabilization. Since in humans CBP/p300 acetylates and stabilizes hGCM1 (ref. 23), we assessed the effects of dCBP in cotransfection assays. dCBP clearly stabilizes GcmFlag (Fig. 4a lanes 1–3, Supplementary Fig. 3a) and the levels of GcmFlag significantly decrease on treatment with the CBP/p300 inhibitor C646 (ref. 24) (Fig. 4a lanes 2–4, Supplementary Fig. 3a). We further analysed the role of acetylation in Gcm stabilization by using the trichostatin (TSA) histone deacetylase (HDAC) inhibitor on cells transfected with a *pAct-gcmFlag* vector alone or with a *pAct-repo* construct (Fig. 4b). TSA treatment increases the levels of GcmFlag compared with those found in non-treated cells (Fig. 4b lanes 1, 2), indicating that the Gcm levels observed in a given cell are the net results of acetylating and deacetylating enzymes. Remarkably, TSA treatment allows the detection of Gcm even in the presence of Repo expression (Fig. 4b lanes 3, 4), suggesting that acetylation counteracts Repo-mediated Gcm degradation. The partial rescue could be due to the fact that the Repo-mediated degradation also involves HDACs that are not affected by TSA, which specifically targets class I and II families of enzymes but not class III HDACs²⁵. Finally, the stabilizing effect of dCBP increases the transcriptional potential of Gcm, as

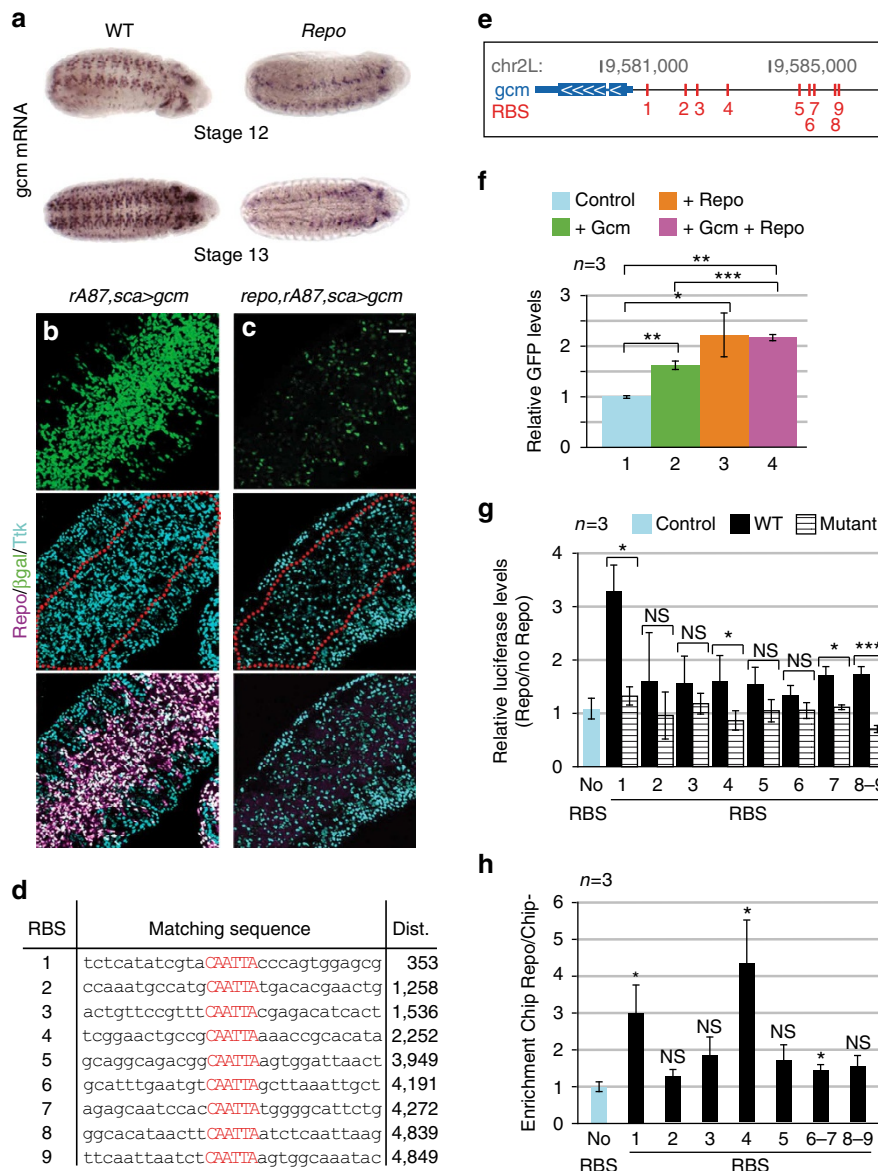


Figure 2 | Repo acts positively on *gcm* expression. (a) *In situ* hybridization with a *gcm* probe. (b) *gcm*^{A87, sca}>*gcm* and (c) *repo, gcm*^{A87, sca}>*gcm* st16 embryos IHC for Repo, βgal, Tramtrack (Ttk, cyan). Red dotted line: VNC. (d) Putative RBSs (in red) on the 6kb-*gcm* promoter. The first column indicates the RBS number, the second column the RBS sequence and the third column shows the distance of the RBS from *gcm* transcription start site. (e) Schematic of the genomic region containing *gcm* and its promoter. The RBSs are represented in red and *gcm* is indicated in blue. (f) Transcriptional effects of Gcm and Repo on the *gcm* promoter. Mean GFP levels standardized against those of βgal (transfection control). WB on total protein extracts from cells transfected with *p6kb-gcm-gal4* + *UAS-GFP* without (column 1 = control) or with *pAct-gcmFlag*, *pAct-repo* or both constructs, quantifications as in Supplementary Information. (g) Activation of *gcm* promoter's RBSs by Repo. Mean luciferase levels standardized against those of βgal (transfection control). Luciferase activity was quantified from cells transfected with the indicated *pGL4.23_RBS*, with or without *pAct-repo*. (h) Binding of Repo on *gcm* promoter. qPCR on Repo ChIP to identify which RBSs in the *gcm* promoter were pulled down with Repo in WT embryos at stage 11.

dCBP–Gcm coexpression leads to a significant increase of reporter gene expression compared with that triggered by Gcm alone (Fig. 4c).

In a more functional perspective, we compared embryos ectopically coexpressing GcmFlag and dCBP to those that ectopically express only GcmFlag. To exclude any negative effect played by Repo, we analysed stage 10 embryos, which do not express Repo yet (Supplementary Fig. 3b,c). WB and IHC analyses show a significant increase of GcmFlag protein levels in embryos coexpressing GcmFlag and dCBP compared with those found in embryos that only ectopically express GcmFlag (Fig. 4d–f).

In sum, dCBP stabilizes Gcm and increases its transcriptional activity.

dCBP acetylates Gcm. Since dCBP acetylates several proteins and histone tails, we asked whether the effects of dCBP on Gcm are direct. We first scored for protein–protein interaction. *Drosophila* and mammalian Gcm proteins show conservation in the domain of hGCM1–CBP physical interaction (Fig. 5a pink boxed sequences) that triggers hGCM1 acetylation²⁶. Immunoprecipitation (IP) assays on transfecting the GcmFlag expression vector show that Gcm and dCBP also interact (Fig. 5c top panel).

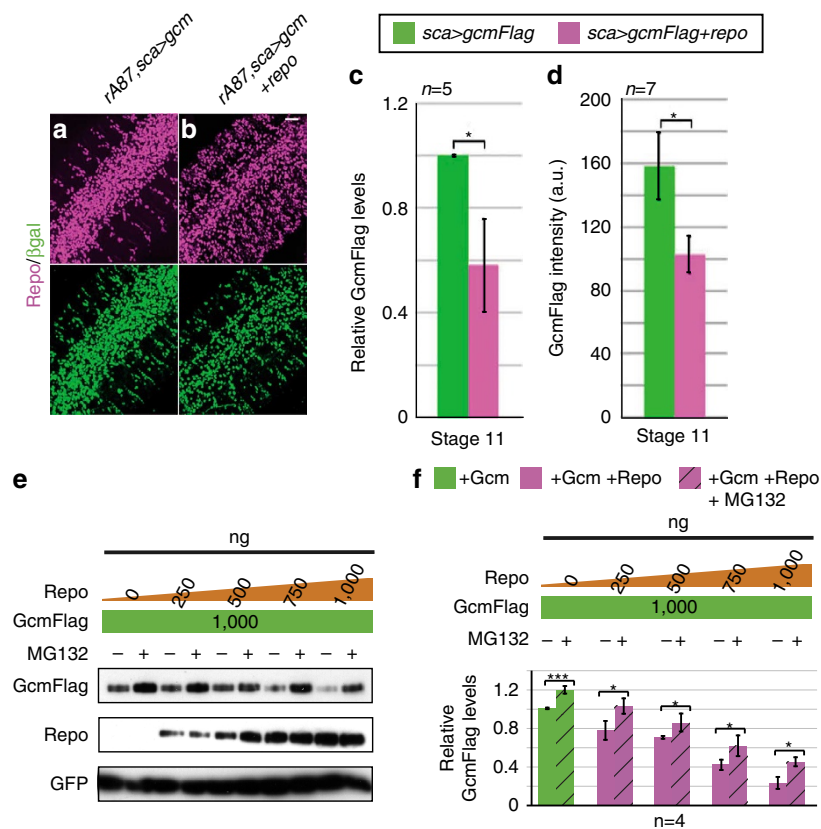


Figure 3 | Repo induces Gcm degradation. (a) $gcm^{A87}, sca > gcm$ and (b) $gcm^{A87}, sca > gcm + repo$ st16 embryos IHC for Repo and βgal . (c) Mean GcmFlag protein levels in $sca > GFP + gcmFlag$ and $sca > GFP + gcmFlag + repo$ embryos, WB with α -Flag. In all WB on embryos, we used α -GFP as a loading control. Because the driver induces transient expression (Supplementary Fig. 2b), we used st11 embryos, which show peak levels of gcm . (d) Quantification of GcmFlag intensity in embryos of the above genotypes (see Supplementary Information). (e) GcmFlag protein degradation on Repo overexpression and treatment with MG132 proteasome inhibitor. WB on total protein extracts from transfected S2 cells using α -Flag for Gcm detection (upper part), α -Repo (middle part) and α -GFP (lower part). Unless specified, the transfection assays aiming at quantifying the Flag used GFP as loading and transfection control ($pAct-gal4, pUAS-GFP$). Quantification is shown in the histogram (f). n , number of assays.

We next scored for dCBP-mediated acetylation. Gcm contains 18 predicted acetylated lysines (K) via CBP/p300 HAT family (ASEB, acetylation set enrichment-based), several of which are conserved throughout evolution and have a high probability of acetylation ($P < 0.05$) (Fig. 5b). We transfected the $pAct-gcmFlag$ vector alone or with dCBP and performed an IP with α -acetyl K (α -Ac): a signal corresponding to the expected GcmFlag molecular weight was specifically detected on the extracts from the Gcm-dCBP expressing cells (Fig. 5c Middle panel). In the same transfection conditions, we performed the IP with α -Flag and WB with α -Ac (Fig. 5c bottom panel lower lanes) and showed that a fraction of GcmFlag is acetylated (Fig. 5c bottom panel upper lanes). The lack of acetylated Gcm on co-IP from S2 cells only expressing Gcm, even though dCBP is endogenously expressed, may be due to the percentage of acetylated Gcm, to dynamic acetylation states and/or to the amount of Gcm present in the total extract used for the IP, too low to be detected by this analysis (see below).

Following this, we assessed the relevance of Gcm acetylation by mutagenesis. To preserve as much as possible the overall protein structure, we limited the mutagenesis to four K residues that present: (i) highest acetylation potential, (ii) most conserved amongst the thirteen insect species for which the genome is available, (iii) presence in hGCM1 (Fig. 5a red encircled asterisks, Fig. 5b sites in bold). We substituted them with arginine (R) residues, as a mimic of not-acetylated K, and found that the

stability of the transfected mutant protein (GcmFlag K > R) severely decreases (Fig. 5d). Furthermore, the transactivation potential of this protein is much weaker than that of the WT one (Fig. 5f). Finally, we tested the impact of acetylation *in vivo*, using transgenic flies that carry a WT or a K > R $UAS-gcmFlag$ construct inserted at the same genomic site, thus avoiding position effects and differences in the expression levels. We crossed the flies with the $sca-gal4$ driver and validated the cell culture data: the WT protein accumulates more (Fig. 5h) and induces more glia (Fig. 5i) than the mutant one, formally demonstrating that acetylation is important for Gcm stability and for gliogenesis. Interestingly, the mutant protein is still stabilized and its transcriptional activity is still potentiated by dCBP, albeit at much lower levels than the WT one (Fig. 5e,g). The mutant protein is also partially active *in vivo*. Thus, other acetylated residues may be relevant as well and/or that other modifications control Gcm activity.

In addition, we mutagenized the same four K sites to glutamine (Q), which in some cases is considered as an acetylation mimicking mutation^{27,28}, expecting a stabilization of the Gcm protein. The mutant protein (GcmFlag K > Q) does accumulate at higher levels compared with the WT, in transfection assays (Fig. 5d). Strikingly, however, it is completely transcriptionally inactive (Fig. 5f), likely due to alteration of the DNA binding property of Gcm, as Q displays different charge and length compared with K²⁸. The presence of dCBP barely changes

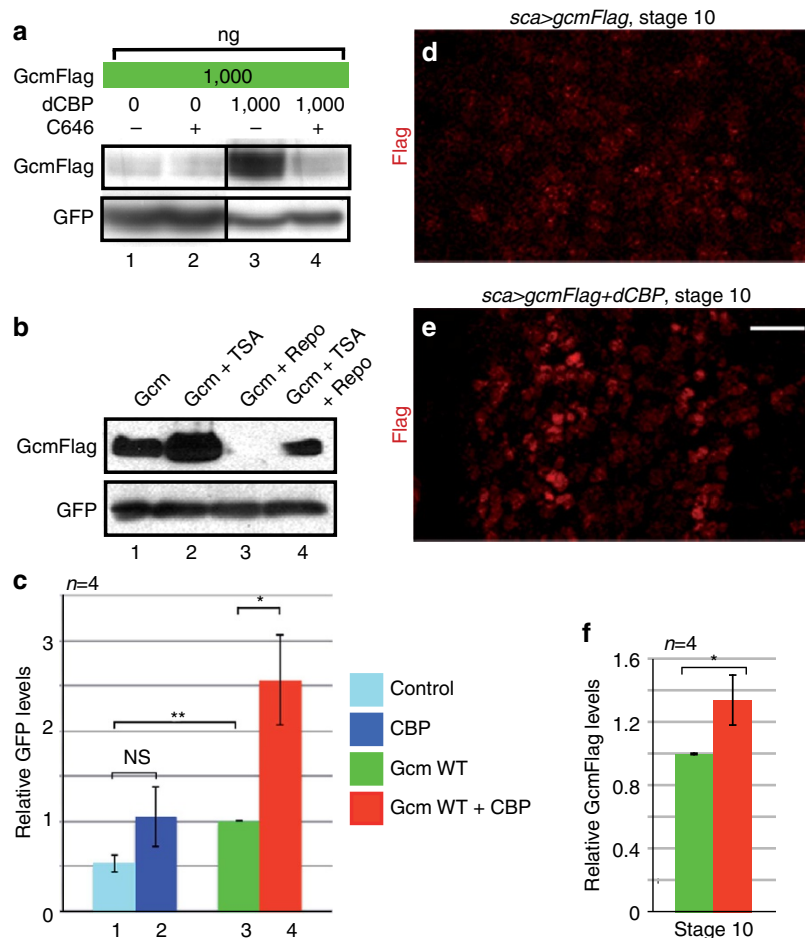


Figure 4 | dCBP stabilizes Gcm in the absence of Repo. (a) Effects of dCBP overexpression on GcmFlag stabilization and treatment with p300/CBP inhibitor C646. WB on total protein extracts from transfected S2 cells using α -Flag (upper lanes) and α -GFP (lower lanes). (b) Effects of HDACs on Gcm stability. WB on total protein extracts from cells transfected with the mentioned expression vectors and treated or not with TSA. (c) Transcriptional effects of Gcm and dCBP on the *6kb-gcm* promoter. WB on total protein extracts on transfection with *pAct-gcmFlag*, *pAct-dCBP* or both constructs. Column 1 and GFP standardization as in Fig. 2f. (d,e) α -Flag IHC on early embryos of the mentioned genotypes. (f) Mean Flag levels on WB from protein extracts of *sca > GFP + gcmFlag* and *sca > GFP + gcmFlag + dCBP* embryos, normalized as above.

the levels of the K>Q protein and does not render it transcriptionally active (Fig. 5e,g). Finally, ectopic expression of a K>Q-targeted transgene shows that the mutations also stabilize the protein and render it inactive *in vivo* (Fig. 5h,i).

To formally demonstrate dCBP-dependent acetylation and identify the acetylated K residue(s), we carried out *in vitro* assays. Two constructs were used, one expressing the first 115 amino acids of the Gcm-DBD (Gcm115) and one extending to amino acid 202 (Gcm202) (Fig. 5a). Only the latter contains the four lysines highly conserved in insect and mammals and predicted to be acetylated: K120, K124, K128 and K179. The WB targeting acetyl lysines revealed that only Gcm202 can be acetylated by dCBP, strongly suggesting that at least one of the four conserved K is acetylated by dCBP, in a dosage-dependent manner (Fig. 5j). Finally, mass spectrometry analysis of the acetylated Gcm202 product clearly demonstrated the acetylation of K128. For the other residues, the current MS techniques are not sufficiently sensitive: K120 was not covered by the analysis; therefore, the acetylation state could not be assessed; K124 was poorly covered and the lateral position of the residue is suboptimal for detecting acetylation; K179, the most covered lysine in the analysis, may still be weakly acetylated (Fig. 5k). The *in vitro* data nevertheless allow us to demonstrate formally that Gcm is acetylated by dCBP, at the resolution of a single lysine residue, K128.

In sum, we show that dCBP acetylates Gcm, that the state of Gcm acetylation regulates its levels and activity, and, importantly, that this controls gliogenesis.

dCBP enhances Gcm degradation in the presence of Repo. The opposite effects of dCBP and Repo on Gcm led us to analyse the tripartite interaction and its possible role on the dynamics of Gcm accumulation. We transfected cells with *pAct-gcmFlag* and *pAct-repo* vectors with or without *pAct-dCBP*. Since the negative effect of Repo on GcmFlag is strong and dosage dependent, we used a ratio of one dose of *pAct-repo* against two doses of *pAct-gcmFlag* and we analysed three conditions: low, medium and high Gcm/Repo expression levels (Fig. 6a columns 1–4, 5–8, 9–12, respectively). Keeping constant the ratio between Gcm and Repo (2:1) allowed us to focus on the impact of absolute protein levels.

At low levels of Gcm and Repo, Gcm is degraded, however, as the amounts of the two proteins increases, Gcm is less degraded (compare green and pink columns at the three concentration conditions in Fig. 6a). This suggests that Gcm and Repo compete for a limiting factor. At low levels of Repo and Gcm, the factor is abundant and Repo efficiently degrades Gcm (Fig. 6a columns 1,2) whereas, at high levels, the factor becomes limiting and Repo no longer degrades Gcm efficiently (Fig. 6a columns 9,10).

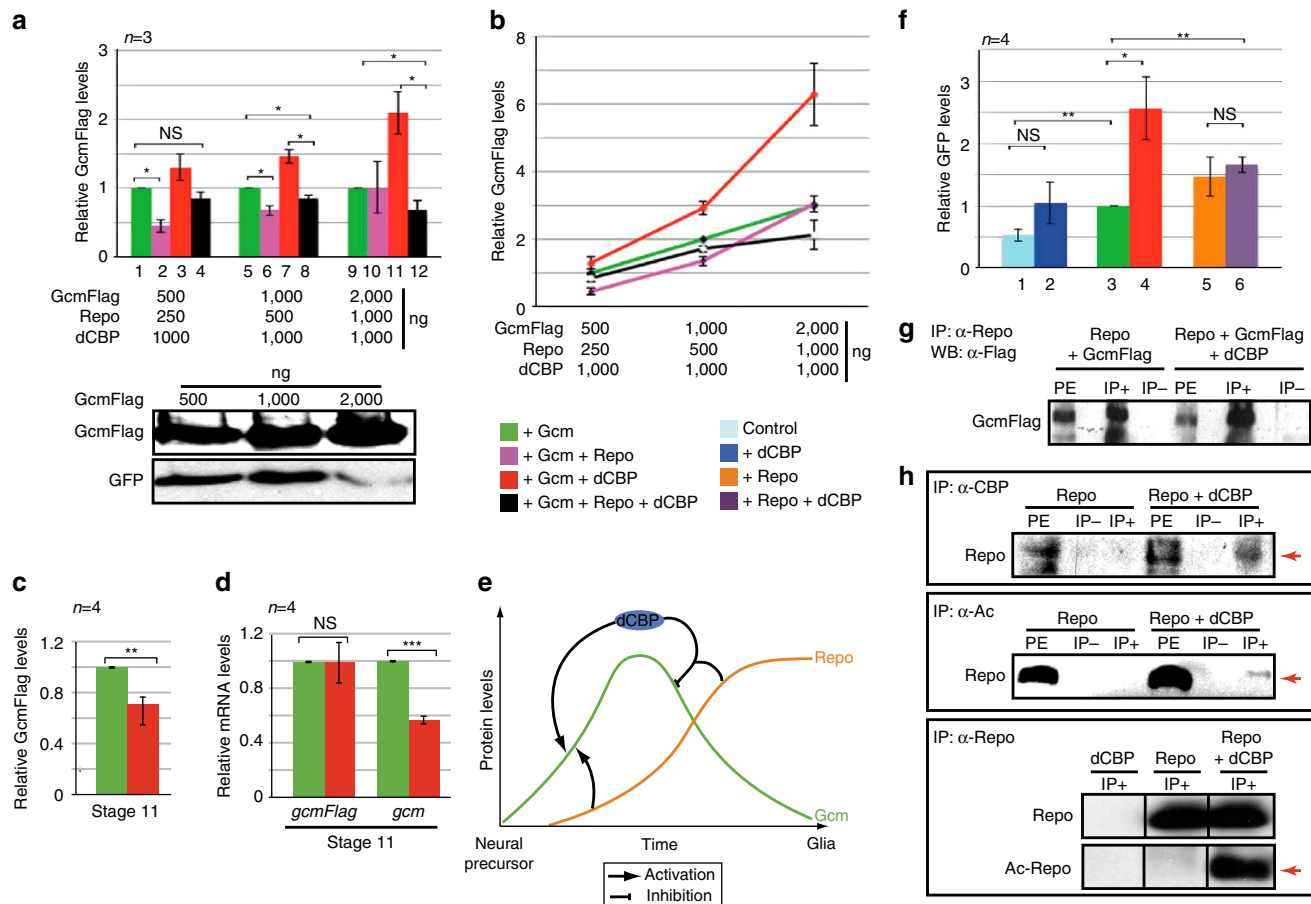


Figure 6 | dCBP enhances Repo-mediated Gcm degradation. (a) Top panel: Flag levels in transfected cells as mentioned in the color-coding legend. All values are relative to those of cells only transfected with *pAct-gcmFlag* (green columns). Mean of three WB normalized as above. Bottom panel: WB showing the Flag levels on transfecting increasing amounts of *pAct-gcmFlag*. (b) Graphical representation of the data in a. Note that here the Flag levels are only normalized against those of GFP. (c) Mean Flag levels on WB from protein extracts of *sca > GFP + gcmFlag* and *sca > GFP + gcmFlag + dCBP* embryos, normalized as above. (d) Mean levels of endogenous (right two columns) and ectopic *gcm* transcripts (*gcmFlag*, left two columns) in *sca > GFP + gcmFlag* and *sca > GFP + gcmFlag + dCBP*, four qPCR assays. (e) Schematics summarizing the regulatory network. (f) Transcriptional effects of dCBP, Gcm and Repo on total protein extracts on transfection with *pAct-gcmFlag*, *pAct-repo*, *pAct-dCBP* alone or in combination. The rest as in Fig. 2f. The first two lanes are the same as those in Fig. 4c. (g) Repo-Gcm interaction with/without dCBP. Protein lysates prepared from cells transfected with the mentioned vectors were subjected to IP with/without α -Repo, WB with α -Flag. (h) Repo-dCBP interaction: IP with α -dCBP, α -Ac, α -Repo on protein lysates from cells transfected with *pAct-repo* with/without *pAct-dCBP*. Symbols as in Fig. 5c. Top panel: IP with/without α -dCBP, WB with α -Repo (red arrow indicates the Repo product). Middle panel: IP with/without α -Ac, WB with α -Repo. Red arrow indicates acetylated Repo. Bottom panel: IP with/without α -Repo, WB with α -Repo (upper lanes) and α -Ac (lower lanes).

The cotransfection assays suggest that dCBP corresponds to the limiting factor (Fig. 6a compare pink and black columns). In the low-level condition, dCBP overexpression partially rescues the negative effect of Repo (Fig. 6a columns 1–4). Thus, dCBP prevents Repo-mediated Gcm degradation. In the medium-level condition, adding dCBP does not seem to rescue the effects of Repo and Gcm levels are decreased compared with Gcm alone transfection (Fig. 6a columns 5–8). Interestingly, in the high-level condition, the effects of dCBP are reversed so that it enhances Gcm degradation in the presence of Repo (Fig. 6a columns 9–12, Fig. 6b compare the behaviour of black, pink lines and red line). Thus, Gcm levels are controlled by a tight equilibrium between Gcm and Repo proteins (Fig. 6b). In sum, the dCBP limiting factor acts positively on the two proteins, thereby triggering opposite effects: direct Gcm stabilization and indirect Gcm destabilization mediated by Repo.

We next analysed stage 11 embryos and tested whether dCBP enhances Gcm degradation in the presence of Repo *in vivo*: animals ectopically coexpressing GcmFlag–dCBP show a significant decrease in the GcmFlag levels compared with those that

ectopically express only GcmFlag (Fig. 6c and Supplementary Fig. 2f right lane).

The decrease of GcmFlag accumulation is not caused by defects in *gcmFlag* transcripts, whose amounts are similar in the two genotypes (Fig. 6d left two columns). As expected, the endogenous *gcm* transcripts show significant reduction in the presence of ectopically expressed dCBP (Fig. 6d right two columns), likely due to the negative control of *gcm* autoregulation. Finally, the negative effects of dCBP could also be explained at least in part by the fact that Gcm and Repo may both need dCBP and compete for their transcriptional activity. Cotransfection assays, however, show that dCBP affects the transcriptional activity of Gcm (enhancement) but not that of Repo, nor does it affect Repo stability (Fig. 6f compare columns 3–4 and 5–6, Supplementary Fig. 3d).

The *in vivo* and the S2 cell data fit well with the dynamic accumulation and the levels of Gcm and Repo observed during gliogenesis (see model in Fig. 6e). At the beginning, Gcm starts accumulating and rapidly reaches threshold levels, via the positive transcriptional and posttranscriptional contribution of dCBP.

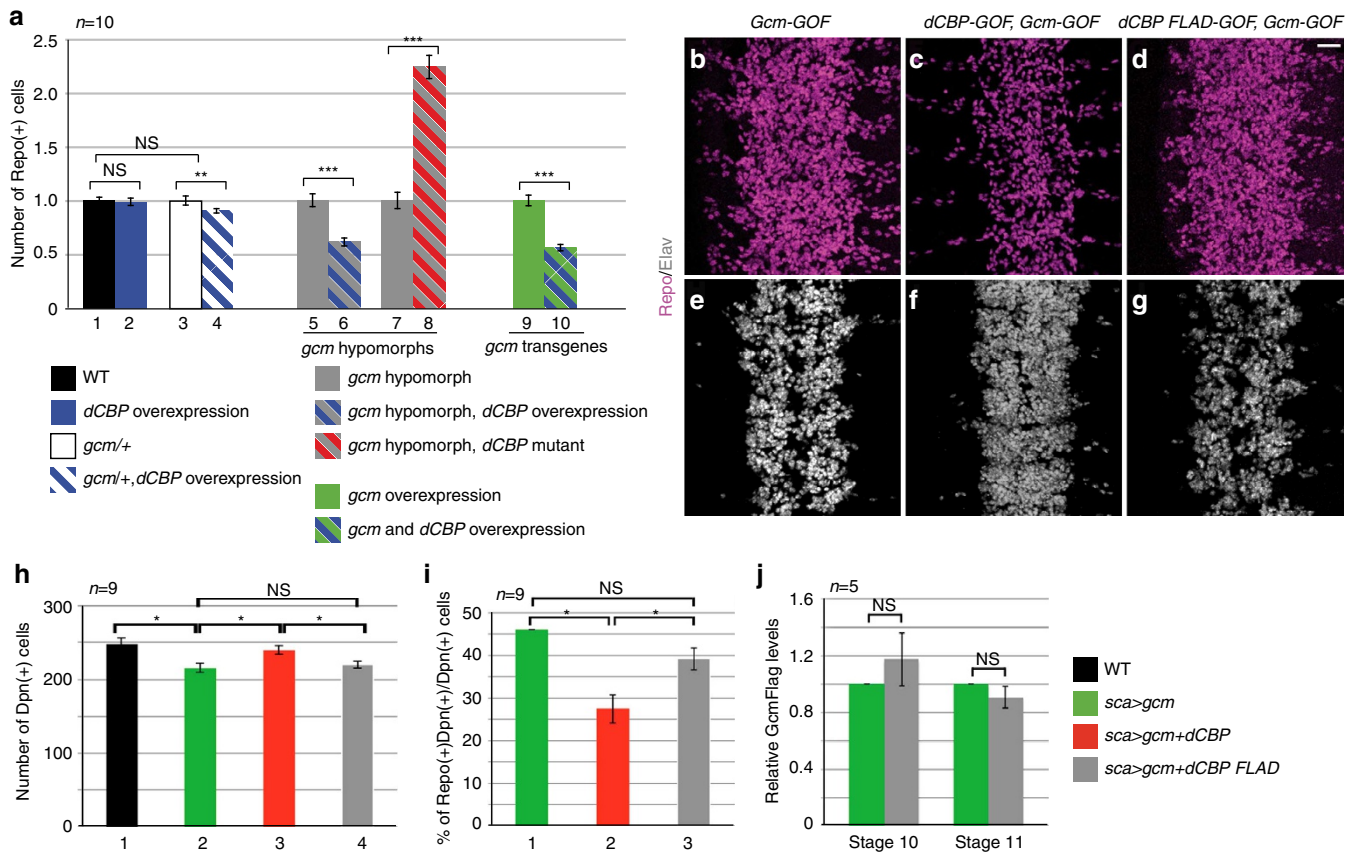


Figure 7 | dCBP HAT inhibits gliogenesis and promotes neuronal differentiation. (a) Number of Repo(+) cells in three segments from the VNC of st16 embryos mutant or ectopically expressing *gcm* and/or *dCBP*. *n*, number of embryos. Note that the absolute number of glia in *gcm*-mutant or overexpressing embryos (grey columns and green column) differs from that of WT embryos (black column). In the genotypes considered as controls, however, the number of glia is brought to 1, for the sake of simplicity. Genotypes as in Supplementary Information. (b–g) St16 embryos IHC for Repo and Elav. (h) Number of Dpn(+) cells in the VNC of st12 embryos and that of Repo(+), Dpn(+) cells in i. (j) Mean Flag levels on WB from embryonic extracts of the mentioned genotypes and stages, normalized as above. *n*, number of assays.

Gcm then activates target genes including Repo and itself, so that both Repo and *Gcm* help building up each other's transcription. As high *Gcm* and Repo levels are reached, *dCBP* facilitates Repo-mediated *Gcm* destruction and *Gcm* fades away, while Repo stays on. This allows terminal glial differentiation.

dCBP facilitates Repo–*Gcm* interaction. The above data suggest that Repo counteracts *Gcm* stability by sequestering *dCBP* and that it destabilizes *Gcm* more efficiently in the presence of *dCBP*. If so, Repo should interact physically with *dCBP* and *Gcm*. IP assays in cells overexpressing Repo alone or together with *dCBP* reveals that the two proteins interact in cells (Fig. 6h top panel) and the complex was also detected in embryos overexpressing *Gcm* (Supplementary Fig. 3e: IP α -Repo, WB α -CBP and vice versa). Repo also directly associates with *Gcm* (Fig. 6g, left side, IP assays using the α -Flag on S2 cells expressing Repo and *Gcm*Flag, note that we used the proteasome inhibitor MG132 to counteract the destabilizing effects of Repo on *Gcm*). In these conditions, simultaneous *dCBP* coexpression does not disrupt Repo–*Gcm* interaction (Fig. 6g, right side). Rather, *dCBP* may facilitate Repo–*Gcm* interaction and increase the ability of Repo to degrade *Gcm* (compare the relative intensity of the signals on IP and in the input to those obtained in the absence of *dCBP*, cells treated in parallel). This is also in line with the WB data (Fig. 6a,b). Together with the fact that acetylation may enhance protein–protein interaction²⁹, these data led us to assess whether *dCBP* mediates the acetylation of Repo, which contains

twenty-seven putative sites, more than fifteen showing a high probability of acetylation and being conserved throughout the thirteen insect genomes (Supplementary Fig. 3f red asterisks). An IP assay for acetylated proteins in cells expressing Repo with or without *dCBP* shows that *dCBP* does mediate Repo acetylation (Fig. 6h middle and bottom panels).

In sum, *dCBP* and Repo are shared components of two interlocked loops (Fig. 6e): on the one hand *dCBP* induces *Gcm* stability, while helping Repo-induced *Gcm* degradation; on the other hand, Repo induces *gcm* expression while mediating *Gcm* degradation.

dCBP-forced expression inhibits gliogenesis and promotes neuronal differentiation. We next analysed the *in vivo* relevance of the outlined network. First, we assessed the impact of *dCBP* levels on endogenous glia. *sca*>*dCBP* embryos contain the same number of glia as *sca*>WT (Fig. 7a) and *dCBP* mutant (*nej*) embryos³⁰. Thus, gliogenesis tolerates fluctuations in the amounts of *dCBP*. Because of the maternal *dCBP* component (Supplementary Fig. 4a–f) and because the whole cascade relies on positive and negative interconnected loops, we used sensitized backgrounds to alter the relative and the absolute amounts of *dCBP* and/or *Gcm*. In these conditions, increasing and decreasing *dCBP* levels aggravates and rescues the *gcm* loss of function phenotype, respectively; thus, *dCBP* represses gliogenesis. Typically, *gcm* heterozygous embryos are like WT embryos, but if they overexpress *dCBP*, they show fewer glia (Fig. 7a

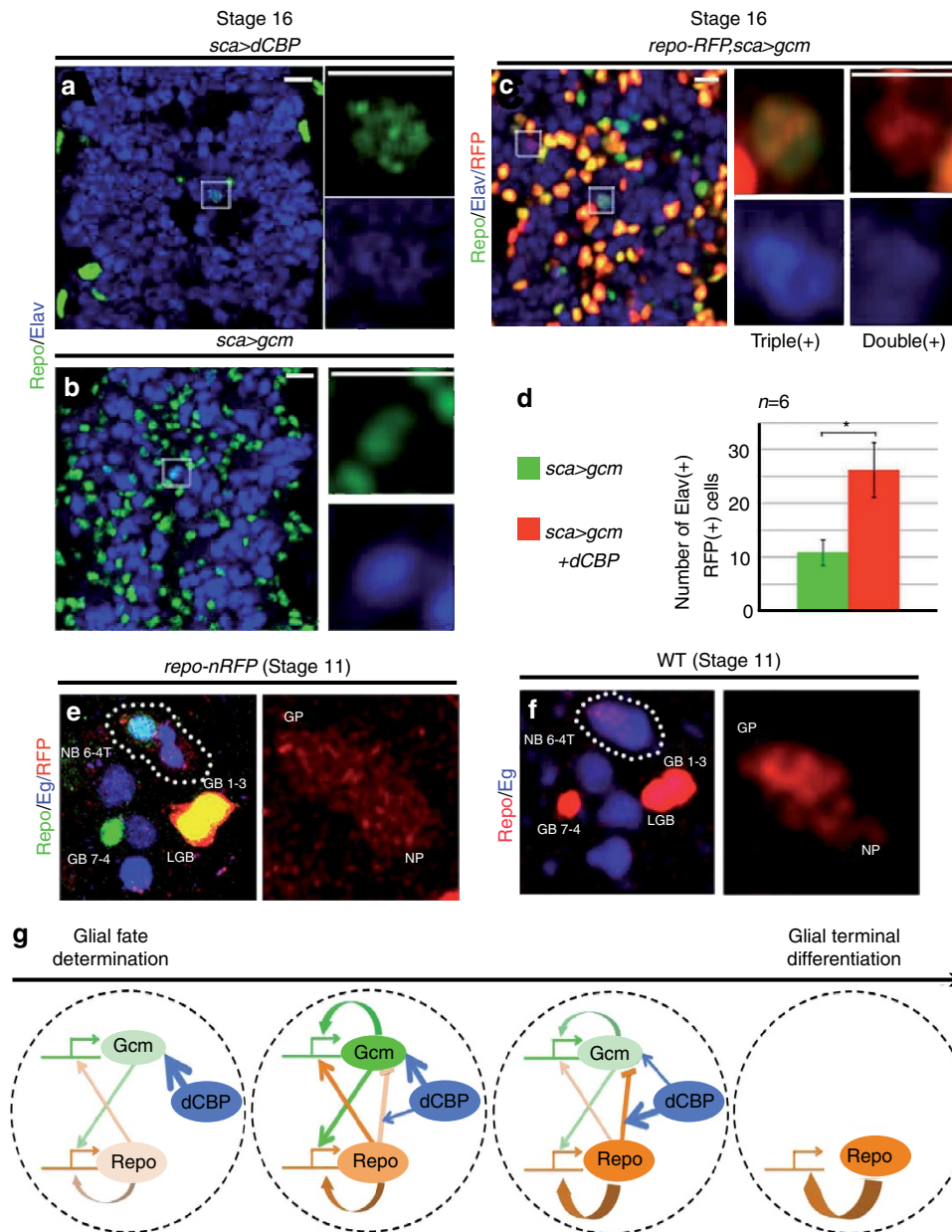


Figure 8 | Glial specification and intermediate fates. (a,b) Optical sections of *sca>dCBP* (a) and *sca>gcm* (b) embryos showing cells weakly coexpressing Repo (green) and Elav (blue). (c) Optical section of Gcm overexpressing embryo carrying the *repo-RFP* glial lineage tracer and labelled for Repo, Elav and RFP. Note the presence of Repo(+), Elav(+), RFP(+) (triple(+)) and Elav(+), RFP(+) cells (double(+)). (d) Number of Elav(+), RFP(+) cells in the whole VNC of st16 embryos. (e) *repo-RFP* embryos labelled with the NB lineage-specific marker Eagle (Eg), Repo and the glial lineage tracer RFP. Dotted line: progenies of the NB6-4T lineage. LGB, GB7-4 and GB1-3 indicate other glial lineages, NP and GP, respectively. (f) WT embryos labelled with Eg and Repo. Dotted line: As above. (g) Detailed sequence of the tripartite interaction. Line and horizontal arrow: Gene and transcription start site, respectively; ellipse: protein; arrow: positive effect; blocked arrow: negative effect.

columns 1–4). Furthermore, dCBP overexpression further reduces the number of glia observed in *gcm* hypomorphic homozygous embryos (Fig. 7a columns 5,6). Similarly, lack of dCBP alleviates the phenotype due to *gcm* hypomorphic mutations (Fig. 7a columns 7,8). The same applies to ectopic glia. The number of ectopic Repo(+) cells is significantly reduced in *sca>gcm + dCBP* compared with that found in *sca>gcm* control embryos (Fig. 7 columns 9,10). In agreement with the hypothesis that altering the Gcm:dCBP ratio breaks the homeostasis, the above phenotypes are dosage dependent (Supplementary Fig. 4k–m). Since dCBP also affects later steps of glial differentiation^{31,32}, we confirmed the early phenotype by analysing a specific lineage. Introducing a *gcm* transgene carrying

its 2 kb promoter region in a *gcm*-null background is sufficient to rescue the birth of the so-called NB1-1 glia¹²; however, *gcm*-mutant embryos carrying the transgene and expressing high dCBP levels show no rescue (Supplementary Fig. 4g–i).

We then assessed how does dCBP affect gliogenesis and found that it impacts on Gcm autoregulation, an important step in the Gcm pathway^{4,12,33}, as the percentage of cells showing *gcm* autoregulation decreases significantly when Gcm and dCBP are ectopically coexpressed (Supplementary Fig. 4j). Since ectopic Gcm works by converting neural stem cells into glia³¹, we analysed the effects of dCBP on this process using the NB marker Deadpan (Dpn). The number of Dpn(+) cells decreases on Gcm expression (Fig. 7h compare black and green columns) and this

phenotype is rescued on Gcm–dCBP coexpression (Fig. 7h red column). Similarly, the number of Dpn(+), Repo(+), NBs, that is, on their way to adopt the glial fate, also decreases on Gcm–dCBP coexpression (Fig. 7i compare red and green columns). Thus, dCBP prevents the ability of Gcm to convert NBs into glia. In line with this (and with the fact that there is less Gcm when dCBP is coexpressed, Fig. 6c) dCBP favors the neuronal programme: *sca > gcm + dCBP* embryos show a higher number of neurons than *sca > gcmFlag* embryos (Fig. 7b,c,e,f). Thus, dCBP promotes neurogenesis and represses gliogenesis in the multipotent precursors. Finally, the acetyltransferase activity of dCBP is required, as none of the above phenotypes (number of glia, neurons, NBs and that of NB on their way to become glia) was observed in coexpression experiments with Gcm and a mutant dCBP transgene (dead HAT dCBP or FLAD³⁰) (Fig. 7d,g–i). Importantly, dCBP FLAD expression does not affect Gcm stability *in vivo* (Fig. 7j).

In sum, the dCBP HAT allows Gcm to produce the appropriate number of glia and neurons from multipotent precursors.

Cell fate building involves an intermediate transient state. The above data show that timely regulation of Gcm controls lineage progression, the event that leads to glial specification. To complete our analysis, we asked whether dCBP affects the very first step of glial specification, that is, the initial choice between the glial and the neuronal fates. Interestingly, forced expression of dCBP induces a rare but fully penetrant phenotype that is absent in WT mature embryos: the coexpression of glial and neuronal markers (Fig. 8a). This suggests that Gcm is expressed below threshold levels, which induces Repo expression very poorly, hence producing cells in which the glial fate cannot be stably implemented and the neuronal fate cannot be stably repressed. Of note, this phenotype also occurs in (few) supernumerary glia induced that likely express ectopic Gcm at suboptimal levels (Fig. 8b). The presence of cells in an intermediate neuronal–glial fate suggests there may also be cells that take the glial fate transiently but then revert to neurons. To prove this, we generated a lineage tracer that would allow us to follow all glial cells.

repo-RFP flies express the stable RFP protein under the control of a *repo* promoter that faithfully reproduces the *repo* expression profile³⁴. RFP is detectable earlier than Repo and later on the two labelling colocalize (Supplementary Fig. 5b). On ectopic Gcm expression, numerous cells display the intermediate fate (triple(+): Elav(+), RFP(+), Repo(+), white arrowheads) or revert to neurons ((double(+): Elav(+), RFP(+), empty arrowheads) (Supplementary Fig. 5a). These phenotypes are also detected at late stages, albeit less numerous (Fig. 8c; Supplementary Fig. 5c). Thus, *repo-RFP* identifies cells that have adopted a stable or a transient glial fate. Interestingly, Gcm–dCBP coexpression enhances the number of presumptive glia that have reverted to neurons cells compared with that found in *sca > gcm* embryos (Fig. 8c,d). Accordingly, the total number of RFP(+) cells and that of Repo(+) alone decreases (Supplementary Fig. 5d).

Finally, we asked whether the ‘frozen’ intermediate fate reflects a situation that occurs transiently during development. The multipotent precursor NB6-4T divides and produces a neuronal precursor (NP) that accumulates *gcm* transcripts at very low levels, and a glial precursor (GP) that accumulates it at high levels^{35,36}. The NP expresses the *repo-RFP* reporter and, more importantly, the Repo protein itself, in a transient manner and at low levels (Fig. 8e,f). Thus, the NP initially expresses an intermediate fate that is normally rapidly suppressed, to give rise to a stable neuronal fate.

In sum, dCBP contributes to the acquisition of the glial fate.

Discussion

Multipotency and lineage specification are the forces that control the generation of specific, stable, fates at the correct number, place and time. We here show that two interlocked and opposing loops control the establishment of the glial fate in the *Drosophila* nervous system. These homeostatic and dynamic processes are triggered by the fate determinant itself, hence ensuring efficient and robust glial differentiation.

While different levels of transcription factors are known to trigger specific fates^{24,37,38}, we here identify temporal regulation as an additional important step. The core of the network is a Gcm–Repo feedback loop. At early stages, the fate determinant Gcm is positively regulated. It induces the expression of the homeodomain protein Repo, which feeds back positively onto *gcm* expression as does Gcm itself. In addition, dCBP stabilizes Gcm via acetylation, similar to the activity of CBP/p300 on other transcription factors, including p53, c-Myc and hGCM1 (refs 23,39). The relevance of Gcm acetylation is also highlighted by the stabilizing effects of the HDAC inhibitor and formally demonstrated by mutagenesis of the acetylation sites. As the Repo protein accumulates, the ratio between the two molecules and their absolute levels change; Repo starts exerting a negative effect on the Gcm protein. Repo represents the ideal trigger of Gcm degradation since (i) it is a Gcm direct target, (ii) is continuously expressed in all glia, (iii) it positively autoregulates, hence becoming independent of Gcm and, finally, (iv) its lack prevents glial terminal differentiation. The role of transcription factors on stimulating the degradation of other factors just starts to emerge. To our knowledge, the only report describing a similar effect concerns the transcription factor STAT2, activated by inflammatory signals, which enhances the proteasomal degradation of RCAN1 (regulator of calcineurin) through the ubiquitin E3 ligase FBW7 (ref. 40).

dCBP enhances the negative effect of Repo on Gcm in cells and *in vivo*. Since dCBP (i) forms a complex with Repo and Gcm, (ii) mediates Repo and Gcm acetylation, (iii) enhances Repo–Gcm interaction as does the inhibition of deacetylation, we speculate that Repo acetylation is necessary for its interaction with Gcm, which then triggers Gcm degradation. This goes along with the findings that dCBP increases Gcm accumulation at stages at which Repo is not expressed and decreases it at stages of Gcm–Repo coexpression.

Thus, homeostatic interactions sequentially move the balance from positive to negative effects and from transcriptional to posttranscriptional pathways. As a consequence, *gcm* expression fades away while *repo* is stably expressed and executes the glial terminal differentiation programme. Disrupting the network affects the number of neurons and glia, in line with the dosage dependence of the *gcm* loss and gain of function phenotypes.

The timely control of Gcm stability emerges as an efficient and fast strategy to produce a robust fate, since the determinant causes its own destruction once it has triggered the novel transcriptional programme. Several mechanisms may account for our findings. (i) Repo may prevent Gcm stability by competing for the same dCBP domain, similar to the competition between STAT2 and p65 for the control of tumour necrosis⁴¹. The idea that dCBP represent a limiting factor is in line with the haploinsufficient phenotype observed in humans¹⁵. (ii) Repo may interact with HDACs that modify and prompt Gcm for degradation. (iii) Repo may interact with E3 ubiquitin ligases. The F-box protein β -TrCP is a p300 interactor⁴² and Ago as well as Slimb, the fly β -TrCP ortholog, mediate Gcm degradation via the proteasome²¹. Regardless of the specific pathway involved, the analysis of discrete phenotypes and sensitized backgrounds combined with the *in vitro* assays allowed us to identify transcriptional and posttranscriptional feedback loops that are

otherwise difficult to dissect. Based on all data, we propose a model for the acquisition of the glial fate (Fig. 8g).

In addition to affecting the number of neurons and glia, altering the interconnected loops generates stable intermediate neuronal/glial fates, a phenotype that was observed in metastatic brain tumours⁴³, implying that ambiguous fates may represent a signature of cancer cells. Interestingly, the intermediate phenotype occurs transiently in natural conditions in the neuronal progeny issued from the neuroGPs. The little amount of Gcm present in these cells is likely eliminated by Repo, thereby producing the neuronal fate. Of note, the neuronal protein Elav was described as being transiently expressed in all embryonic glial lineages at early stages⁴⁴, suggesting that an analogous process occurs in the glial progeny. Hence, bidirectional interactions and balance between a fate determinant, its target and a widely expressed HAT ensure the dynamic levels of Gcm that induces a stable glial identity.

Interestingly, the so-called epithelial–mesenchymal transition (EMT), which triggers heart morphogenesis, mesoderm and neural crest formation in vertebrates, also involves intermediate, transient, phenotypes referred to as metastable states⁴⁵. EMT depends on transcription factors including Twist and Snail, whose activity is quantitatively regulated at the level of protein stability^{46,47}. Little is known about how the transiently expressed Twist protein regulates EMT during embryonic development. Interestingly, however, *Drosophila* Twist triggers the mesodermal fate, which is stabilized by the evolutionarily conserved dMef2 protein⁴⁸. This homeodomain containing protein and Twist cross and autoregulate transcriptionally. Given that vertebrate Twist is highly expressed in tumours and has an essential role in metastasis⁴⁹, it will be interesting to determine whether a homeostatic balance similar to the one working in the Gcm pathway also applies to Twist.

In sum, our work identifies the molecular pathway controlling glial specification, paving the way for future work on other developmental pathways. Understanding whether intermediate states have been underscored due to their transient nature may clarify pathological phenotypes such as those observed in cancer.

Methods

Drosophila strains. *w¹¹¹⁸* was the WT. Transgenic lines were: *UAS-gcm* (*F18A* (one transgene) = *weak-gcm*; *M24A* (two transgenes) = *strong-gcm*)¹⁶, *gcm^{rA87}/CyO* (*weak hypomorph*), *gcm³⁴/CyO, twi-LacZ* (*hypomorph*), *gcm²⁶/CyO, twi-LacZ* (null), *Df(2L)132/CyO, twi-LacZ* (null allele)^{2,3}; *repo³⁶⁹²/TM3Ubx-lacZ*; *UAS-gcmFlag; UAS-repo¹¹; UAS-dCBP* and *UAS-CBP FLAD³⁰; 2kb-gcm¹²; nej³* (*dCBP null*)⁵⁰; *UAS-GFP, hs-gal4*, and *sca-gal4* (*BDSC*). The *gcm* hypomorphic combinations shown in Supplementary Fig. 4k,l are: *gcm^{rA87}/gcm²⁶* (*weak*), *gcm³⁴/gcm³⁴* (*medium*, same as columns 7,8 Fig. 7a), *gcm³⁴/Df(2L)132* (*strong*, same as columns 5,6 Fig. 7a). The medium *UAS-gcm* transgene in Supplementary Fig. 4m (and Fig. 7a *gcm* transgenes) was *RS1*³¹. The *repo-RFP* line carries 4.3kb promoter of the *repo* gene fused with the RFP coding sequence. This fragment recapitulates the expression profile of the endogenous *repo* gene³⁴. To compare the protein levels on Gcm mutagenesis, three lines were generated by targeted transgenesis into the ZH-attP-68E genomic site (III chromosome)⁵¹: *UAS-gcmFlag*, *UAS-gcmFlag K>R* and *UAS-gcmFlag K>Q*.

IHC and in situ hybridization. Overnight or staged embryos were dechorionated in bleach for 5 min, rinsed in water, fixed in 50% heptane/50% PEM-formaldehyde for 25 min and devitellinized in methanol/heptane for 1 min. The *in situ* hybridization was carried out using a probe DIG-*gcm* [1:100]^{52,53}. For the immunolabelling, the embryos were rinsed in methanol, in phosphate-buffered saline (PBS) 0.3% Triton X-100, and incubated in blocking reagent (Roche) for 30 min at room temperature (RT). The embryos were incubated with primary antibody in blocking reagent overnight at 4 °C, washed in PBS 3 × 10 min at RT, incubated with secondary antibodies for 2 h at RT and washed 3 × 10 min at RT⁵². The embryos were mounted in Vectashield (Vector #H-1000) and analysed by conventional (Zeiss Axiophot) or confocal microscopy (SP5 Leica confocal microscope). Antibodies were as follows: mouse (m)- α -Repo (1:50) and rat (rt)- α -Elav (1:200) from DSHB; chicken (ck)- α -GFP (1:1,000); rabbit (rb)- α -RFP (1:500) and rb- α -Flag (Abcam); rb- α -GFP (1:500) (Molecular Probes); rb- α - β -gal (1:500, Cappel); rb- α -Eagle [1:500]⁵⁴; guinea pig- α -Deadpan (1:1,000, J. Skeath);

rt- α -Ttk69 [1:1,000]⁵⁵. Secondary antibodies were FITC-, Cy3-, Cy5-conjugated (1:400, Jackson).

Cell counting. Using Imaris Bitplane, the following parameters were followed: (1) three-dimensional masks were generated along the z-stacks of the embryonic ventral nerve cord (VNC) as regions of interest; (2) the number of cells was identified using the following parameters: select 'Enable smooth', surface area detail = 0.5, select 'Enable eliminate background', diameter of largest sphere = 5 μ m, threshold = 30, region growing estimated diameter = 3, region growing background subtraction = true, quality above 10, number of voxels above 10. The false negative is eliminated manually using Imaris tool on three-dimensional visualization of the VNC. Mean and s.e.m. were calculated for all genotypes and samples were subjected to *t*-test.

Protein intensity measurement. GcmFlag and GFP intensity measurements were done by ImageJ tool²⁰. Masks were generated as region of interest for a defined area in the VNC of embryo the z-stack (10 μ m), and the fluorescence intensities (pixel number) were measured and summed for all sections. The resulted intensities were subjected to *t*-test.

qPCR analysis and mutagenesis. Staged embryos were collected from the different genotypes. Total RNA was purified using Trizol (Invitrogen), reverse transcribed by SuperScript II and the qPCR was done with the Roche LightCycler480 and Sybr Green Master mix (Roche). Expression levels were automatically calculated (LightCycler480 Software, release 1.5.0) by calibration to gene-specific standard curves generated on input cDNAs³¹. Collected values were normalized to *GFP* messenger RNA amount, derived from four amplification reactions, each performed on four independent experiments. Primers are in Supplementary Table 1.

Cell culture and transfection assays. *Drosophila* S2 cells were cultured in Schneider's medium (Fisher Scientific). Cells (6×10^6) were cultured in 6-well plates 12 h before transfection. Each well was transfected with expression vectors: *pActin-gcmFlag* (*pAct-gcmFlag*)²¹, *pActin-repo* (*pAct-repo*)¹¹, *pActin-dCBP* (*pAct-dCBP*)⁵⁰, *pActin-lacZ* (*pAct-lacZ*), *pActin-gal4* (*pAct-gal4*), *pUAST-eGFP* (*pUAS-GFP*), *p6kb-gcm-gal4*, as indicated using 10 μ l per 1 μ g of DNA of Lipofectamine (Sigma). When required, *pAct* vector was added as carrier. Forty-eight hours post transfection, cells were lysed. Transfection efficiencies were normalized as specified in the legend to β -gal or GFP. Each experiment was performed at least three times. For drug treatments, 45 h post transfection, cells were treated 3 h with 20 μ M of the proteasome inhibitor MG132 (Sigma), 30 μ M of CBP/p300 inhibitor C646 (BioVision) or 30 μ M Trichostatin (Sigma) cells.

Immunoblot analysis. Proteins were extracted from staged embryos from the specified genotypes³¹. A total of 30 μ g of protein was separated by 8% SDS-PAGE gel, transferred onto nitrocellulose membrane and probed with primary antibodies diluted in 1 × PBS, 3% milk: m- α -Flag (1:5,000) (Sigma), ck- α -GFP (1:5,000) (Abcam), m- α - β -gal (1:1,000), m- α -Repo (1:2,000) (DSHB), rb- α -dCBP (1:5,000) (M. Mannervik). Signal was detected using the Pierce ECL western blotting substrate (Thermo Fisher Scientific) using HRP-conjugated secondary antibodies (1:5,000, Jackson). Chemiluminescence detection was performed according to manufacturer's instructions (Amersham). Band quantifications used the ImageJ software. Gels submenu was used as indicated in ImageJ website. Results were compared using *t*-test.

Full blots of each WB presented in the figures are presented in Supplementary Fig. 6.

Immunoprecipitation. Transfected cells or staged embryos were lysed in the IP buffer (25 mM Tris-HCl pH 7.9, 10% (v/v) glycerol, 0.1% NP-40, 0.5 mM DTT, 5 mM MgCl₂, 1 × proteinase inhibitor cocktail (Roche)). Protein lysates were immunoprecipitated with 100 μ l protein G-Sepharose, for polyclonal dCBP antibody (Sigma), or A-Sepharose, for monoclonal Flag and Repo antibodies and ~5 μ g of the different antibodies (as indicated). G/A-Sepharose protein-antibody-protein complexes were washed three times with the IP buffer comprising 0.5 M KCl and twice with buffer containing 100 mM KCl. After washing, protein-G-antibody-bound proteins were boiled in SDS sample buffer and analysed by WB. Acetylation was detected using rb- α -Ac-K (Cell Signaling #9441).

Luciferase assay. Double-stranded oligonucleotides covering the RBS of *gcm* promoter were synthesized. RBS 8 and RBS 9 were combined on the same oligonucleotide. Each oligonucleotide was designed with the WT RBS CAATTA and with a mutated RBS CAGTTA not bound by Repo¹¹ (Supplementary Table 2). For each RBS, the double-stranded oligonucleotide was digested with 20 U of KpnI (NEB #R3142S) and 20 U of NheI (NEB #R3131S) in Cutsmart buffer (NEB #B7204S) for 1 h 30 min at 37 °C. The digested probe was cleaned using the PCR clean-up kit (MN #740609).

A quantity of 1 µg of luciferase reporter plasmid *pGL4.23[luc2/minP]* (*pGL4.23*) (Promega #E841A) was digested with KpnI and NheI as described previously, after 1 h 30 min at 37 °C, 20 U of CIP (Promega #M0290S) were added to the plasmid and incubated for 1 h at 37 °C. The plasmid was cleaned using the PCR clean-up kit (MN #740609). A quantity of 50 ng of digested luciferase plasmid was combined with the digested annealed probes (ratio plasmid:probe = 1:6), 400 U of ligase (NEB #M0202S) and ligation buffer (NEB #B0202S) and incubated overnight at 18 °C. The ligated plasmids were then dialysed for 30 min on membrane filters (Millipore #VSWP02500) and amplified using the Plasmid DNA purification kit (MN #740410) according to manufacturer's instructions.

Transfections of S2 cells were carried out in 12-well plates using Effectene transfection reagent (Qiagen #301427). Cells were transfected with 0.5 µg *pAct-lacZ*, 0.5 µg *pGL4.23* carrying the indicated RBS (or empty for the negative control), 0.5 µg *pAct-repo* or 0.5 µg *pAct*. Forty-eight hours after transfection, the cells were collected, washed once in cold PBS and resuspended in 100 µl of lysis buffer (25 mM Tris-phosphate pH7.8, 2 mM EDTA, 1 mM DTT, 10% glycerol, 1% Triton X-100). The suspensions were frozen/thawed four times in liquid nitrogen and centrifuged 30 min at 4 °C at 13,000g.

The activities of the Luciferase and the LacZ were measured in triplicate for each sample. For the LacZ measurement, 20 µl of lysate was mixed with 50 µl of βgal assay buffer (60 mM Na₂PO₄, 40 mM NaH₂PO₄, 10 mM KCl, 1 mM MgCl₂, 50 mM β-mercaptoethanol) and 20 µl ONPG (4 mg ml⁻¹) and incubated at 37 °C for 20 min. The reaction was stopped by adding 50 µl 1 M Na₂CO₃ and the DO at 415 nm was measured. For the Luciferase activity, 10 µl of protein lysate was analysed on an opaque 96-well plate (Packard Instrument #6005290) with a Berthold MicroLuminat LB96P Luminometer by injecting 50 µl of luciferase buffer (20 mM Tris-phosphate pH 7.8, 1 mM MgCl₂, 2.5 mM MgSO₄, 0.1 mM EDTA, 0.5 mM ATP, 0.5 mM luciferin, 0.3 mM coenzyme A, 30 mM DTT). For both LacZ assay and Luciferase assay, the level of the background was estimated using lysate from S2 cells not transfected. The relative Luciferase levels were calculated as follows: the background was subtracted from each value, then the average of the technical triplicate were calculated. From there, the Luciferase activity of each sample was normalized to the LacZ activity (Luciferase activity/LacZ activity) to correct for transfection efficiency variability and the ratio (Luciferase with Repo/Luciferase without Repo) was calculated. For each RBS WT and mutant, biological triplicates were carried out.

Repo chromatin IP. The chromatin IP (ChIP) was performed according to standard protocols^{56,57} with modification. A quantity of 100 mg of embryos *w¹¹¹⁸* stage 11 was homogenized with a Dounce homogenizer in 1 × PBS, 0.4% formaldehyde and incubated 10 min at RT. Glycine was added to 0.2 M, the chromatin was incubated 10 min at RT and centrifuged 5 min at 500g at 4 °C. The pellet was rinsed with cold PBS and resuspended in sonication buffer (50 mM HEPES pH8, 140 mM NaCl, 1 mM EDTA, 1% Triton X-100, 0.1% Na-deoxycholate, 0.25% SDS, 0.5 mM phenylmethanesulphonyl fluoride (PMSF), 1 × protease inhibitor complex) and incubated 5 min on ice. The lysate was sonicated 2 × 15 min (30 s on/30 s off) with a Diagenode water bath sonicator and centrifuged 15 min at 13,000g at 4 °C. The supernatant was diluted 2.5 times in dilution buffer (15 mM Tris-HCl pH8, 150 mM NaCl, 1 mM EDTA, 1% Triton X-100, 0.1% SDS), 50 µg of diluted chromatin were used per ChIP. The chromatin solution was precleared 2 h at 4 °C with 40 µl of protein A Sepharose beads (Sigma #p3391) blocked with salmon sperm and BSA then centrifuged at 1,000g for 5 min. The supernatant was incubated overnight at 4 °C with agitation with 5 µg of mouse anti-Repo antibody (DSHB #8D12) or with 5 µg of mouse IgG for the negative control; 40 µl of blocked protein-A Sepharose beads were added to the chromatin and incubated 1 h at 4 °C with agitation. The beads were pelleted 2 min at 500g at 4 °C and washed twice 10 min with the following buffer: low-salt wash buffer (20 mM Tris pH8, 150 mM NaCl, 2 mM EDTA, 1% Triton X-100, 0.1% SDS), high-salt wash buffer (20 mM Tris pH8, 500 mM NaCl, 2 mM EDTA, 1% Triton X-100, 0.1% SDS), LiCl wash buffer (10 mM Tris pH8, 1 mM EDTA, 0.25 M LiCl, 1% Na-deoxycholate, 1% NP-40) and TE buffer. The chromatin was eluted twice 15 min at RT with 250 µl elution buffer (100 mM NaHCO₃, 1% SDS), 20 µl of NaCl 5M was added and the chromatin was incubated at 65 °C overnight, then 10 µg RNase A was added and incubated for 1 h at 37 °C and 20 µg of proteinase K, 10 µl Tris-HCl pH6.8 2M and 10 µl EDTA 0.5M were added and incubated 1 h at 42 °C. The DNA was extracted with phenol/chloroform and resuspended in 20 µl water. A quantity of 5 ng of chromatin were used per qPCR using SYBR Green (Roche) in 10 µl with primers targeting each RBS of *gcm* promoter and primers designed in a region of *gcm2* carrying no RBS for a negative control (Supplementary Table 3). The enrichment was calculated for each RBS with the following formula: $2^{(Ct_{Chip_IgG} - Ct_{Chip_Repo})}$. Three biological replicates were done.

Electrophoretic mobility shift assays. *hs-gal4 > gcm* synchronized embryos were submitted to 1-h heat-shock at 37 °C ((4–5 h) after egg laying) and raised to differentiate 6 h at 25 °C. Embryos were collected in Schneider's medium, 3 mM EDTA and dissociated (Wheaton Dounce homogenizer). Cell suspensions were obtained on centrifugation (100g, 5 min). Cells were washed with 1 × PBS and incubated 10 min at 4 °C in buffer A (10 mM HEPES-KOH pH 7.9, 1.5 mM MgCl₂, 10 mM KCl, 0.5 mM DTT, 0.2 mM PMSF). After centrifugation of 10 s, the pellet was resuspended in buffer C (20 mM HEPES-KOH pH 7.9, 25% glycerol, 420 mM

NaCl, 1.5 mM MgCl₂, 0.2 mM EDTA, 0.5 mM DTT, 0.2 mM PMSF) for high salt extraction. Cellular debris were removed by centrifugation for 2 min at 4 °C and DNA binding proteins were stored at –80 °C. The profile of Repo was verified by WB analysis. Around 10 µg of nuclear extract was used in binding assays¹².

RBS 1 probe: 5'-TCTCATATCGTACAATTACCCAGTGGAGCG-3'.

Mutagenesis of GcmFlag lysines. GcmFlag sequence was mutated as follows: K120R, K124R, K128R and K179R (K > R mutations) or K120Q, K124Q, K128Q and K179Q (K > Q mutations) using *pAct-gcmFlag*²¹ as template. For each mutant, three segments were synthesized separately (primers in Supplementary Table 4). For each segment, PCRs were done on 50 ng of *pAct-gcmFlag* using Expand High fidelity PCR system (Roche #11732641001) and the PCR programme: 94 °C 2 min, (94 °C 15 s, 50 °C 30 s, 72 °C 1 min 30 s) × 25 cycles and 72 °C 7 min. The segments were extracted from 1% agarose gel using Nucleospin PCR clean-up (MN #740609). The three segments were combined in equimolar concentration and a second round of PCR was performed with the primers 'first segment K > R forward' and 'third segment K > R reverse', using the Expand High fidelity PCR system with the following PCR programme: 94 °C 2 min, (94 °C 15 s, 45 °C 30 s, 72 °C 1 min 30 s) × 5 cycles, (94 °C 15 s, 55 °C 30 s, 72 °C 1 min 30 s) × 25 cycles and 72 °C 7 min. The PCR products *gcmFlag* K > R of around 1.8 kb were gel extracted as above.

The PCR products *gcmFlag* K > R and *gcmFlag* K > Q were digested with 20 U EcoRI-HF (NEB #R3101S) and 20 U XbaI (NEB #R0145S) overnight at 37 °C in NEB buffer 2 (NEB #B7002S). Restriction enzymes were heat inactivated at 65 °C 20 min and the PCR product was cleaned with Nucleospin PCR clean-up. The plasmids *pUAST* and *pAct* were digested with EcoRI and XbaI as described previously and treated with CIP (NEB #M0290S) according to manufacturer's instructions. The digested plasmids were purified using Nucleospin PCR clean-up.

The ligations were carried out overnight at 18 °C with 50 ng of digested plasmids and 100 ng of digested PCR products *gcmFlag* K > R or *gcmFlag* K > Q using T4 DNA ligase (NEB #M0202S) according to the manufacturer's instruction. The ligation products were dialyzed on 0.025 MF mixed cellulose ester membrane (Millipore #VSWP02500), electroporated into DH5α competent cells and isolated using NucleoSpin Plasmid kit. The integrity of the sequences of *gcmFlag* K > R and *gcmFlag* K > Q was assessed by Sanger sequencing using the primers: *pUAST_F* (5'-taaccagcaaccaagtaaatc-3') and *pUAST_R* (5'-ctccatcatcagttccat-3'), the primers first segment K > R Forward and third segment reverse for the *pPAC5C*.

Mutated GcmFlag stability and activity. S2 cells were transfected with 1 µg of one of the following expression vectors: *pUAS-gcmFlag* K > R, *pUAS-gcmFlag* K > Q, *pUAS-gcmFlag* and with 1 µg of *pUAS-lacZ*, 1 µg of *pAct-gal4* and 1 µg of *4.3kb-repo-GFP*¹⁴ using the Effectene transfection reagent (Qiagen). Forty-eight hours post transfection, the cells were collected, lysed in 25 mM Tris-HCl pH 7.9, 10% glycerol, 0.1% NP-40, 0.5 mM DTT, 5 mM MgCl₂, 1 × protease inhibitor (Roche #11836153001), frozen-thawed four times in liquid nitrogen and centrifuged at 13,000g 10 min at 4 °C. The supernatant was collected, its concentration was measured using nanodrop and immunoblots were performed with 50 µg of protein of each sample, primary antibody targeting Flag (1:5,000) (Sigma), GFP (1:5,000) (Abcam) and β-gal (1:1,000) and HRP-conjugated secondary antibodies, as described previously.

Each transfection was performed at least three times, the results were compared using *t*-test.

Mutated GcmFlag stability and activity in presence of CBP. *Drosophila* S2 cells were transfected with 1 µg of one of the following expression vectors: *pAct-gcmFlag* K > R, *pAct-gcmFlag* K > Q, *pAct-gcmFlag* and with 1 µg of *pAct-lacZ*, 1 µg of *4.3kb-repo-GFP*¹⁴ and in CBP + samples 1 µg of *pAct-dCBP*⁵⁰ using the Effectene transfection reagent (Qiagen #301427). When required, the *pAct* vector was added as carrier. Forty-eight hours post transfection, GFP-positive cells were counted using ImageJ tools, then the cells were collected, lysed in 25 mM Tris-HCl pH 7.9, 10% glycerol, 0.1% NP-40, 0.5 mM DTT, 5 mM MgCl₂, 1 × protease inhibitor (Roche #11836153001), frozen-thawed four times in liquid nitrogen and centrifuged at 13,000g 10 min at 4 °C. The supernatant was collected, its concentration was measured using nanodrop and immunoblots were performed with 50 µg of protein of each sample, primary antibody targeting Flag (1:5,000) (Sigma), GFP (1:5,000) (Abcam) and β-gal (1:1,000) and HRP-conjugated secondary antibodies, as described previously. Each transfection was performed at least three times and the results were compared using *t*-test.

In vitro acetylation and mass spectrometry analysis. The CBP HAT domain, GST-dCBP 1675–2510, was produced in BL21 cells, purified on glutathione sepharose beads⁵⁸ and eluted with thrombin. Similarly, sequences encoding the 115 first amino acids (Gcm115) and 202 first amino acids of Gcm (Gcm202) were cloned in *pGex4T3* vector⁴ produced in BL21 cells and bound to glutathione sepharose beads. The *in vitro* acetylation was carried out directly on the beads with 1 µg or 4 µg purified CBP in 5% glycerol, 50 mM NaCl, 50 mM Tris pH8, 0.1 mM EDTA, 10 mM Na-butyrate, 1 mM DTT, 1 × protease inhibitor complex Roche #04693116001, 30 µM acetyl-coenzyme A for 1 h at 30 °C⁵⁹. The beads carrying Gcm-DBD 115 aa or Gcm-DBD 202 aa were washed twice with PBS and eluted

with 1 U of thrombin overnight at RT. The eluted proteins were analysed by WB targeting acetylated lysine.

Acetylated Gcm202 was analysed by mass spectrometry to identify the acetylated lysines. The protein band was excised from a 15% SDS-PAGE coloured by Coomassie blue, digested with chymotrypsin (Promega) or ArgC (Roche) and analysed with a Hybrid Ion Trap-Orbitrap Mass Spectrometer coupled with a nanoRSLC system (ThermoScientific). The protocol is detailed in Supplementary Methods .

References

- Campos-Ortega, J. A. Mechanisms of early neurogenesis in *Drosophila melanogaster*. *J. Neurobiol.* **24**, 1305–1327 (1993).
- Hosoya, T., Takizawa, K., Nitta, K. & Hotta, Y. Glial cells missing: a binary switch between neuronal and glial determination in *Drosophila*. *Cell* **82**, 1025–1036 (1995).
- Jones, B. W., Fetter, R. D., Tear, G. & Goodman, C. S. Glial cells missing: a genetic switch that controls glial versus neuronal fate. *Cell* **82**, 1013–1023 (1995).
- Miller, A. A., Bernardoni, R. & Giangrande, A. Positive autoregulation of the glial promoting factor glide/gcm. *EMBO J.* **17**, 6316–6326 (1998).
- Vincent, S., Vonesch, J. L. & Giangrande, A. Glide directs glial fate commitment and cell fate switch between neurones and glia. *Development* **122**, 131–139 (1996).
- Altenhein, B. *et al.* Expression profiling of glial genes during *Drosophila* embryogenesis. *Dev. Biol.* **296**, 545–560 (2006).
- Egger, B. *et al.* Gliogenesis in *Drosophila*: genome-wide analysis of downstream genes of glial cells missing in the embryonic nervous system. *Development* **129**, 3295–3309 (2002).
- Freeman, M. R., Delrow, J., Kim, J., Johnson, E. & Doe, C. Q. Unwrapping glial biology: Gcm target genes regulating glial development, diversification, and function. *Neuron* **38**, 567–580 (2003).
- Halter, D. A. *et al.* The homeobox gene repo is required for the differentiation and maintenance of glia function in the embryonic nervous system of *Drosophila melanogaster*. *Development* **121**, 317–332 (1995).
- Xiong, W. C., Okano, H., Patel, N. H., Blendy, J. A. & Montell, C. Repo encodes a glial-specific homeo domain protein required in the *Drosophila* nervous system. *Genes Dev.* **8**, 981–994 (1994).
- Yuasa, Y. *et al.* *Drosophila* homeodomain protein REPO controls glial differentiation by cooperating with ETS and BTB transcription factors. *Development* **130**, 2419–2428 (2003).
- De Iaco, R. *et al.* Hucklebein-mediated autoregulation of Glide/Gcm triggers glia specification. *EMBO J.* **25**, 244–254 (2006).
- Campbell, G. *et al.* RK2, a glial-specific homeodomain protein required for embryonic nerve cord condensation and viability in *Drosophila*. *Development* **120**, 2957–2966 (1994).
- Laneve, P. *et al.* The Gcm/Glide molecular and cellular pathway: new actors and new lineages. *Dev. Biol.* **375**, 65–78 (2013).
- Bedford, D. C. & Brindle, P. K. Is histone acetylation the most important physiological function for CBP and p300? *Aging (Albany NY)* **4**, 247–255 (2012).
- Bernardoni, R., Miller, A. A. & Giangrande, A. Glial differentiation does not require a neural ground state. *Development* **125**, 3189–3200 (1998).
- Leibovitch, B. A. *et al.* GAGA factor and the TFIID complex collaborate in generating an open chromatin structure at the *Drosophila melanogaster* hsp26 promoter. *Mol. Cell Biol.* **22**, 6148–6157 (2002).
- Wu, J. *et al.* Diverse histone modifications on histone 3 lysine 9 and their relation to DNA methylation in specifying gene silencing. *BMC Genomics* **8**, 131 (2007).
- Yang, X. *et al.* miR-449a and miR-449b are direct transcriptional targets of E2F1 and negatively regulate pRb-E2F1 activity through a feedback loop by targeting CDK6 and CDC25A. *Genes Dev.* **23**, 2388–2393 (2009).
- Burgess, A. *et al.* Loss of human Greatwall results in G2 arrest and multiple mitotic defects due to deregulation of the cyclin B-Cdc2/PP2A balance. *Proc Natl Acad Sci USA* **107**, 12564–12569 (2010).
- Ho, M. S. *et al.* Gcm protein degradation suppresses proliferation of glial progenitors. *Proc. Natl Acad. Sci. USA* **106**, 6778–6783 (2009).
- Vierstra, R. D. The ubiquitin-26S proteasome system at the nexus of plant biology. *Nat. Rev. Mol. Cell Biol.* **10**, 385–397 (2009).
- Chang, C. W., Chuang, H. C., Yu, C., Yao, T. P. & Chen, H. Stimulation of GCMA transcriptional activity by cyclic AMP/protein kinase A signaling is attributed to CBP-mediated acetylation of GCMA. *Mol. Cell Biol.* **25**, 8401–8414 (2005).
- Bowers, E. M. *et al.* Virtual ligand screening of the p300/CBP histone acetyltransferase: identification of a selective small molecule inhibitor. *Chem. Biol.* **17**, 471–482 (2010).
- Vanhaecke, T., Papeleu, P., Elaut, G. & Rogiers, V. Trichostatin A-like hydroxamate histone deacetylase inhibitors as therapeutic agents: toxicological point of view. *Curr. Med. Chem.* **11**, 1629–1643 (2004).
- Wang, H. & Chia, W. *Drosophila* neural progenitor polarity and asymmetric division. *Biol. Cell* **97**, 63–74 (2005).
- Fujimoto, H. *et al.* A possible overestimation of the effect of acetylation on lysine residues in KQ mutant analysis. *J. Comput. Chem.* **33**, 239–246 (2012).
- Kamieniarz, K. & Schneider, R. Tools to tackle protein acetylation. *Chem. Biol.* **16**, 1027–1029 (2009).
- Nguyen, D. X., Baglia, L. A., Huang, S. M., Baker, C. M. & McCance, D. J. Acetylation regulates the differentiation-specific functions of the retinoblastoma protein. *EMBO J.* **23**, 1609–1618 (2004).
- Kumar, J. P., Jamal, T., Doetsch, A., Turner, F. R. & Duffy, J. B. CREB binding protein functions during successive stages of eye development in *Drosophila*. *Genetics* **168**, 877–893 (2004).
- Flici, H. *et al.* Gcm/Glide-dependent conversion into glia depends on neural stem cell age, but not on division, triggering a chromatin signature that is conserved in vertebrate glia. *Development* **138**, 4167–4178 (2011).
- Schmidt, I. *et al.* Transcriptional regulation of peripheral glial cell differentiation in the embryonic nervous system of *Drosophila*. *Glia* **59**, 1264–1272 (2011).
- Popkova, A. *et al.* Polycomb controls gliogenesis by regulating the transient expression of the Gcm/Glide fate determinant. *PLoS Genet.* **8**, e1003159 (2012).
- Lee, B. P. & Jones, B. W. Transcriptional regulation of the *Drosophila* glial gene repo. *Mech. Dev.* **122**, 849–862 (2005).
- Akiyama-Oda, Y., Hosoya, T. & Hotta, Y. Asymmetric cell division of thoracic neuroblast 6-4 to bifurcate glial and neuronal lineage in *Drosophila*. *Development* **126**, 1967–1974 (1999).
- Bernardoni, R., Kammerer, M., Vonesch, J. L. & Giangrande, A. Gliogenesis depends on glide/gcm through asymmetric division of neuroglioblasts. *Dev. Biol.* **216**, 265–275 (1999).
- Grueber, W. B., Jan, L. Y. & Jan, Y. N. Different levels of the homeodomain protein cut regulate distinct dendrite branching patterns of *Drosophila* multidendritic neurons. *Cell* **112**, 805–818 (2003).
- Jin, H. *et al.* Runx1 regulates embryonic myeloid fate choice in zebrafish through a negative feedback loop inhibiting Pu.1 expression. *Blood* **119**, 5239–5249 (2012).
- Bedford, DC., Kasper, LH., Fukuyama, T. & Brindle, PK. Target gene context influences the transcriptional requirement for the KAT3 family of CBP and p300 histone acetyltransferases. *Epigenetics* **5**, 9–15 (2010).
- Lee, J. W. *et al.* The transcription factor STAT2 enhances proteasomal degradation of RCAN1 through the ubiquitin E3 ligase FBW7. *Biochem. Biophys. Res. Commun.* **420**, 404–410 (2012).
- Hottiger, M. O., Felzien, L. K. & Nabel, G. J. Modulation of cytokine-induced HIV gene expression by competitive binding of transcription factors to the coactivator p300. *EMBO J.* **17**, 3124–3134 (1998).
- Kimrel, E. A. & Kung, A. L. The F-box protein beta-TrCp1/Fbw1a interacts with p300 to enhance beta-catenin transcriptional activity. *J. Biol. Chem.* **284**, 13033–13044 (2009).
- Beaucher, M. *et al.* *Drosophila* brain tumor metastases express both neuronal and glial cell type markers. *Dev. Biol.* **301**, 287–297 (2007).
- Berger, C., Renner, S., Luer, K. & Technau, G. M. The commonly used marker ELAV is transiently expressed in neuroblasts and glial cells in the *Drosophila* embryonic CNS. *Dev. Dyn.* **236**, 3562–3568 (2007).
- Yang, J. & Weinberg, R. A. Epithelial-mesenchymal transition: at the crossroads of development and tumor metastasis. *Dev. Cell* **14**, 818–829 (2008).
- Lander, R., Nordin, K. & LaBonne, C. The F-box protein Ppa is a common regulator of core EMT factors Twist, Snail, Slug, and Sip1. *J. Cell Biol.* **194**, 17–25 (2011).
- Zhang, K. *et al.* Lats2 kinase potentiates Snail1 activity by promoting nuclear retention upon phosphorylation. *EMBO J.* **31**, 29–43 (2012).
- Cripps, R. M. *et al.* The myogenic regulatory gene Mef2 is a direct target for transcriptional activation by Twist during *Drosophila* myogenesis. *Genes Dev.* **12**, 422–434 (1998).
- Yang, J. *et al.* Twist, a master regulator of morphogenesis, plays an essential role in tumor metastasis. *Cell* **117**, 927–939 (2004).
- Akimaru, H. *et al.* *Drosophila* CBP is a co-activator of cubitus interruptus in hedgehog signalling. *Nature* **386**, 735–738 (1997).
- Bischof, J., Maeda, R. K., Hediger, M., Karch, F. & Basler, K. An optimized transgenesis system for *Drosophila* using germ-line-specific phiC31 integrases. *Proc. Natl Acad. Sci. USA* **104**, 3312–3317 (2007).
- Bernardoni, R., Vivancos, V. & Giangrande, A. Glide/gcm is expressed and required in the scavenger cell lineage. *Dev. Biol.* **191**, 118–130 (1997).
- Lehmann, R. & Tautz, D. In situ hybridization to RNA. *Methods Cell Biol.* **44**, 575–598 (1994).
- Dittrich, R., Bossing, T., Gould, AP., Technau, GM. & Urban, J. The differentiation of the serotonergic neurons in the *Drosophila* ventral nerve cord depends on the combined function of the zinc finger proteins Eagle and Hucklebein. *Development* **124**, 2515–2525 (1997).

55. Giesen, K. *et al.* Glial development in the *Drosophila* CNS requires concomitant activation of glial and repression of neuronal differentiation genes. *Development* **124**, 2307–2316 (1997).
56. Delacroix, L. *et al.* Cell-specific interaction of retinoic acid receptors with target genes in mouse embryonic fibroblasts and embryonic stem cells. *Mol. Cell. Biol.* **30**, 231–244 (2010).
57. Martianov, I. *et al.* Cell-specific occupancy of an extended repertoire of CREM and CREB binding loci in male germ cells. *BMC Genomics* **11**, 530 (2010).
58. Lilja, T., Aihara, H., Stabell, M., Nibu, Y. & Mannervik, M. The acetyltransferase activity of *Drosophila* CBP is dispensable for regulation of the Dpp pathway in the early embryo. *Dev. Biol.* **305**, 650–658 (2007).
59. Tropberger, P. *et al.* Regulation of transcription through acetylation of H3K122 on the lateral surface of the histone octamer. *Cell* **152**, 859–872 (2013).

Acknowledgements

We thank J. Skeath, J. Kumar, M. Mannervik, C. Gonzalez, B. Altenhein, B.J. Jones, the Bloomington Stock Center for reagents and all lab members for suggestions. We thank Pei-Yi Chen for help with mutant constructs, C. Diebold, C. Delaporte, N. Arbogast and H. Dietrich for technical assistance, as well as the imaging, the cell culture and the mass spectrometry facilities. We thank C. Romier for advice on the 3D structure of the Gcm-DBD and on the mutagenesis. This work was supported by: Institut National de la Santé et de la Recherche Médicale, Centre National de la Recherche Scientifique, Université de Strasbourg, Hôpital de Strasbourg, Association pour la Recherche sur le Cancer, Institut National du Cancer, Agence Nationale de la Recherche (ANR) and

Région Alsace. F.H., O.K., P.L. and S.B. were supported by FRM fellowships, B.E. by ARC, P.B.C. by ANR and Neurex Network (TriNeuron Programme Interreg IV Upper Rhine). The work was also supported by the grant ANR-10-LABX-0030-INRT, a French State fund managed by the *Agence Nationale de la Recherche* under the frame programme *Investissements d'Avenir* labelled ANR-10-IDEX-0002-02.

Author contributions

A.G., H.F., P.B.C., O.K. conceived and designed the experiments. P.B.C., H.F., O.K., P.L., O.F.K., B.E. performed the experiments. A.G., P.B.C., H.F., O.K., P.L., O.F.K., B.E. analysed the data. S.B., H.R. contributed reagents/materials/analysis tools. A.G., H.F., P.B.C., O.K., P.L. wrote the paper.

Additional information

Supplementary Information accompanies this paper at <http://www.nature.com/naturecommunications>

Competing financial interests: The authors declare no competing financial interests.

Reprints and permission information is available online at <http://npg.nature.com/reprintsandpermissions/>

How to cite this article: Flici, H. *et al.* Interlocked loops trigger lineage specification and stable fates in the *Drosophila* nervous system. *Nat. Commun.* 5:4484 doi: 10.1038/ncomms5484 (2014).